Numerical Methods in Civil Engineering

Evaluation of 2D concentrically braced frames with cylindrical dampers subjected to near-field earthquake ground motions

Masoud Mirtaheri [*], Mojtaba Salkhordeh[**], S. Mehdi S. Kolbadi[***], Hamid Mirzaeefard[****], Mohammad R. Razzaghian[*****]

ARTICLE INFO

Article history:
Received:
January 2020.
Revised:
February 2020.
Accepted:
March 2020.

Keywords:
Steel structures
Cylindrical friction dampers
Near field earth quacks
Incremental dynamic analysis.

Abstract:

Near field earthquakes have imposed major damage to buildings in the past years. In some cases, the intensity of such damage is too considerable to be disregarded. The most effective way to improve seismic performance of buildings is applying a seismic control technique. The cylindrical friction damper is one of these methods, which has become popular for its desirable performance in the energy dissipation of lateral loads. The main objective of this study is to evaluate the near-field seismic performance of braced frame buildings equipped with cylindrical friction dampers. In this regard, four steel braced frame buildings, including a 4-, 8-, 12-, and 16-story braced frame building are modeled in OpenSees platform. Then, a set of near-field earthquake motions are applied to these structures and the structural response is captured in each story. Results show that there is a direct relation between the optimal slip load and the intensity of the input earthquake. In the next step, the structures are analyzed by selecting the optimum slip load for the damper. It is revealed that cylindrical friction dampers improved structural performance in terms of energy absorption of the structure. However, findings confirm that there is an indirect relationship between the number of floors in a building and the above mentioned feature of these dampers.

1. Introduction

Structures developed for high earthquake-prone regions should possess two criteria. First, the structures need to have satisfying solidity as to control lateral displacement [1]. As such, it brings about a decrease in the number of seismic or non-seismic damage over repeated but medium severity earthquakes. Secondly, they should have satisfying resistance and plasticity in order to withstand devastating earthquakes. Slight and non-structural damage is allowed [2].

When a near field earthquake happens tremendous energy due to available pulse in relevant ground motion record is created, which leads to develop strike-type forces. In fact, vertical elements are more serious than that of horizontal in these strikes. A cylindrical friction damper acts like a fuse and prevents buckling of braces. Therefore, the maximum slip load which the frame is about to carry should be less than the critical buckling load of the braces. Under the system, the dissipation of energy is transformed from joints of the developed plastic as the main part of the structure to a secondary part, which leads to an increase in deformation of plastic and damage. A cylindrical friction damper has a complete geometrical axial symmetry that not only simplifies calculations but also fixates pressure force or vertical pressure on friction surfaces. In this kind of damper, pressure force between friction surfaces is equal in all of its parts. In addition, symmetry forces between surfaces is also equal and do not change as time passes by, which increases reliability of the system [3,4].

** Corresponding Author: Associated professor, Department of Civil and Environmental Engineering, K. N. Toosi University of Technology, Tehran, Iran. Email: mmirtaheri@kntu.ac.ir*
*** PhD student, Department of Civil and Environmental Engineering, K. N. Toosi University of Technology, Tehran, Iran.*
**** PhD student, Department of Civil and Environmental Engineering, K. N. Toosi University of Technology, Tehran, Iran.*
***** PhD student, Department of Civil and Environmental Engineering, K. N. Toosi University of Technology, Tehran, Iran.*
****** Graduate student, Department of Civil and Environmental Engineering, K. N. Toosi University of Technology, Tehran, Iran.*

Different types of energy dissipation devices are proposed and experimented for mitigating the seismic performance of buildings, and more are still being investigated. Frictional dampers dissipate energy through friction created by two solid bodies sliding relative to each other. Pall and Marsh [5] presented frictional dampers applied at the crossing joint of the X brace. Tension in one of the braces forces the joint to slip, thus activating four links that in turn force the joint in the other brace to slip. This damper is called the Pall frictional damper (PFD). Wu et al. [6] proposed improved Pall frictional damper (IPFD), which replicates the mechanical properties of the PFD, but offers some advantages in terms of ease of manufacture and assembly. Sumitomo friction damper [7] utilizes a more complicated design. The pre-compressed internal spring exerts a force that is converted through the action of inner and outer wedges into a normal force on the friction pads. Fluor Daniel Inc. explored and experimented another type of friction device called Energy Dissipating Restraint (EDR) [8]. Mirtaheri et al proposed the cylindrical friction damper for the purpose of improving seismic performance of steel buildings [3].

In recent years, a large number of research has been implemented for the purpose of seismic retrofit of buildings [9]. Ahmad et al (2020) proposed a cost effective base-isolation system to mitigate the seismic performance of buildings [10]. Lavan et al (2014) proposed a seismic retrofitting method based on the application of viscous damper with optimum size and location in the structure [11].

This paper investigates the application of cylindrical friction damper in steel braced frame buildings subjected to near and far field earthquakes. A comparative study is implemented to compare the efficiency of the proposed damper in the structures subjected to near and far field earthquakes. A parametric study is applied to determine the optimum slip load of damper for both near and far field earthquakes. Results show a promising improvement of seismic performance of buildings equipped with this damper in terms of energy dissipation and inter-story drift ratio reduction.

2. Material and Methods

2.1 Modelling procedure

As can be seen from Figure 1, a typical n-story frame with three ports having a diagonal brace in its medium port has been developed using ETABS software. The following hypotheses were put forward to develop the model and conduct analyses. All the buildings considered for implementing the present study were modeled and designed based on Iranian Code of Practice for Seismic Resistant Design of Buildings; Standard No. 2800, 4rd [12]. In this research, ST37 steel was used. Structures were developed on a ground of type II, and the height of all stories was three meters. The two dimensional frame had three ports and the length of each one was five meters. In order to support geometrical non-linear behavior of braces, one thousandth of the element length in the middle of each one has been considered as eccentricity. It is worth noting that it brings buckling into the brace.

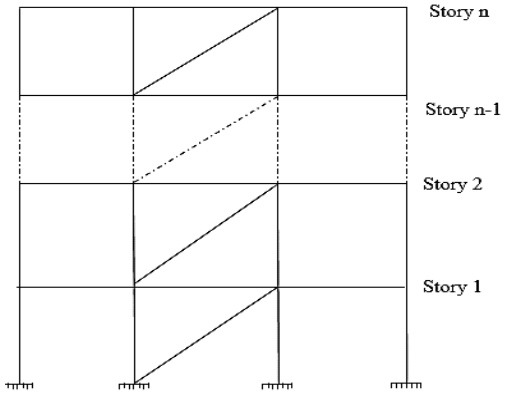

Fig. 1: Modelling a three port, n-story frame with a diagonal brace in the medium port using ETABS software

Fiber elements were used in section of columns, bars, and braces. Threads were selected appropriate to material used in order to provide the structure plasticity and, by way of illustration, elastoplastic threads were applied by taking solidity into account. Bars, columns, and braces were developed using STEEL 02 constitutive material model. A leaning column was modeled to apply the P-delta effect in 2D models. To do so, a column with lateral stiffness of zero and nodal gravity load equal to the eliminated gravity loads for each story was defined next to the frame. This column was connected to the frame with truss element with significant stiffness to apply the effect of P-delta from the column to the frame. For the cylindrical friction damper, two node links which simply accept axial forces were introduced into the OpenSees software and developed by making the use of STEEL 01. The behavior of such material is defined as a bilinear curve by considering the strain-hardening corresponding to the behavior of steel material. Figure 2 illustrates chart of force or pressure regarding displacement or strain in these materials [10].

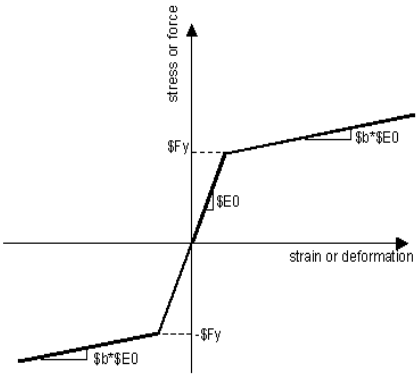

Fig. 2: Graph of force or pressure based on strain or displacement in Steel01 using OpenSees software

In the loading cycle, the hysteresis curve turns to a rectangular curve, which confirms collected data of samples. It should be mentioned that the brace element is modeled with 8 sub-elements, which assign a sinusoidal curve with maximum imperfection of $l/1000$ (l is the length of the brace element) to allow the braces to buckle at their critical buckling load. P-delta geometric transform is assigned to the column elements, and corotational geometric transform is assigned to all beams. It is worth noting that the gravity loads are applied to the beams as a uniform load along their length. Behavior of symmetric structures in the current research was approximate to two dimensional extracted frames (structures were of three ports and each port was five meters in length). Therefore, one of the middle frames was extracted from three dimensional structures and modeled using OpenSees software [13,14].

In the model, the damper and brace were developed in series. Since the amount of both buckling and surrender forces were assumed greater than dampers' slip force, the deformation of the brace could be disregarded compared to that of the damper. By the same token, solidity of the brace needs to be much greater than that of the damper ($K_b \gg K_d$). Equivalent stiffness of the modelled brace and damper is as follows:

$$\frac{1}{K_e} = \frac{1}{K_b} + \frac{1}{K_d} \quad (1)$$

Where:

Ke: is equivalent solidity of both brace and damper

Kb: is solidity of the brace

Kd: is solidity of the damper

So, we identify:

$$K_e = \frac{K_b K_d}{K_b + K_d} \quad (2)$$

Consequently,

$$K_e = \lim_{K_b \to \infty} \frac{K_b K_d}{K_b + K_d} = K_d \quad (3)$$

So, the equivalent solidity and damper solidity are viewed equal [15].

2.2. Features of earthquakes

Table 1 and 2 depict ground motion record of near and far-field earthquakes, respectively, in which, collected data is comprised of information such as earthquake number, Richter scale, year in which earthquake occurred, name of earthquake, name of recording station, and finally its owner. These near fault motions cover a moment magnitude range from 6.2 to 7.5 and a rupture distance (closest distance from site to fault rupture plane) range from 0.0 to 8:9 km [16,17,21].

Table 1. ground motion record concerning far-field earthquakes

Far Field					
ID	Earthquake			Recording Station	
NO.	M	Year	Name	Name	Owner
1	6.5	1979	Imperial Valley	Elcentro Array #11	USGS
2	7.3	1992	Landers	Coolwater	SCE
3	6.7	1994	Northridge	Beverly Hills-Mulhol	USC
4	7.6	1999	Chi-Chi, Taiwan	CHY 101	CWB
5	7.1	1999	Duzce, Turkey	Bolu	ERD
6	6.9	1989	Loma Prieta	Capitola	CDMG
7	7.5	1999	Kocaeli, Turkey	Arcelik	KOERI

Table 2. ground motion record concerning near-field earthquakes

Near Field With Pulse					
ID	Earthquake			Recording Station	
NO.	M	Year	Name	Name	Owner
1	6.5	1979	Imperial Valley-06	Elcentro Array #7	USGS
2	7.3	1992	Landers	Lucerne	SCE
3	6.7	1994	Northridge-01	Sylmar-Olive View	CDMG
4	7.6	1999	Chi-Chi, Taiwan	TCU102	CWB
5	7.1	1999	Duzce, Turkey	Duzce	ERD
6	6.9	1989	Loma Prieta	Saratoga-Aloha	CDMG
7	7.5	1999	Kocaeli, Turkey	Izmit	ERD

The spectrum of heptad ground motion records regarding near and far-field earthquakes, as well as collected data about comparison of these earthquakes with the sample are shown in figures 3, 4, 5, and 6. At intervals of 0.2T and 1.5T, the acceleration of compared seismic spectrums do not necessarily have to be less than that of the sample earthquake (T is referred as the structure interval (s)) [15].

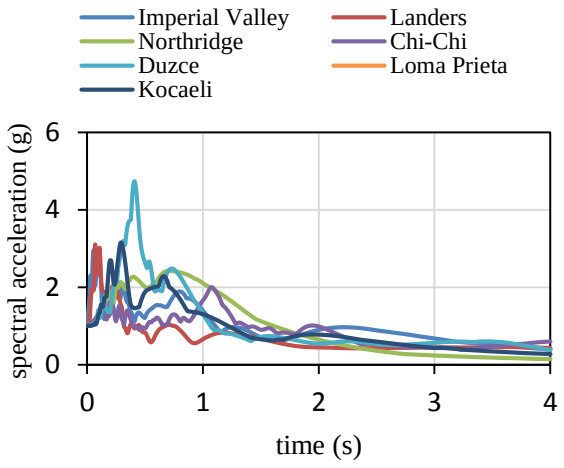

Fig. 3: Spectral acceleration regarding ground motion record of a near-field earthquake.

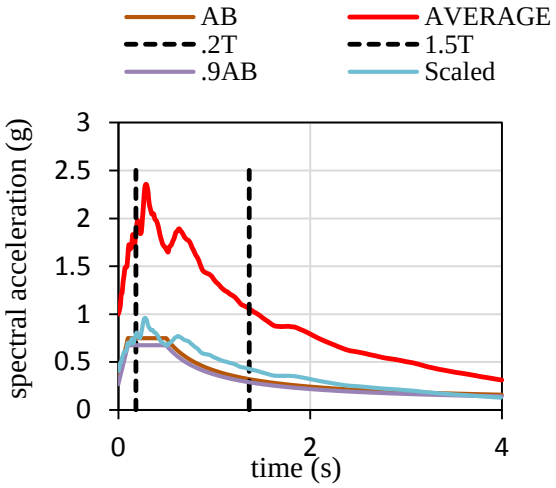

Fig. 4: spectral acceleration of a near-field earthquake in comparison with that of the sample earthquake

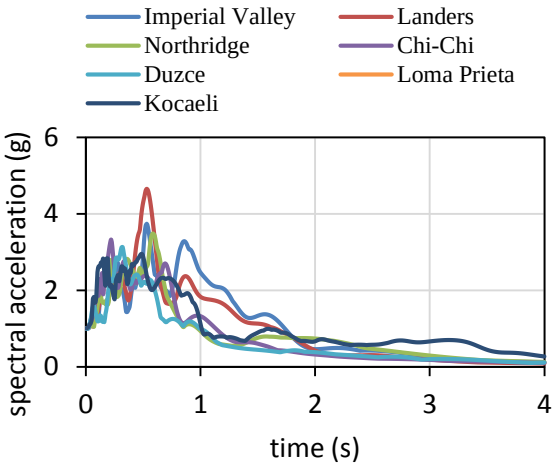

Fig. 5: Spectral acceleration obtained from ground motion record of a far-field earthquake.

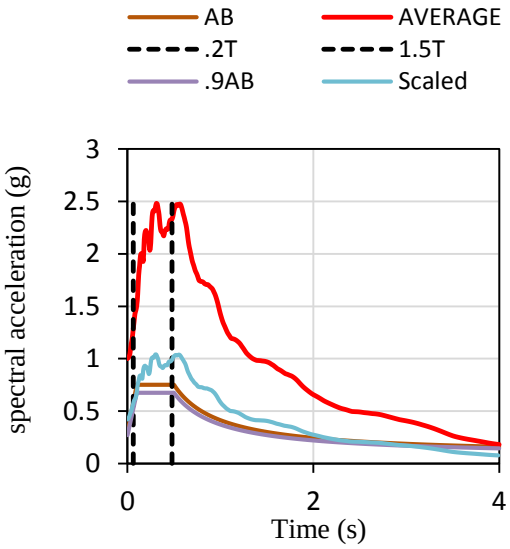

Fig. 6: Spectral acceleration obtained from ground motion record of a far-field earthquake in comparison with the sample

3. Results and discussion

3.1. The optimum slip load

Figure 7 illustrates roof displacement in terms of various slip forces of damper. As can be seen from the figure, first of all, the slip force is assumed to be 80 percent of buckling force of the brace. Then, roof displacement is calculated using the given value. As a result, values obtained for roof displacement as well as slip force depict a point in the curve, and then the diagram is developed by linking the points. Generally speaking, slip force which creates the least roof displacement is called optimum slip load [19].

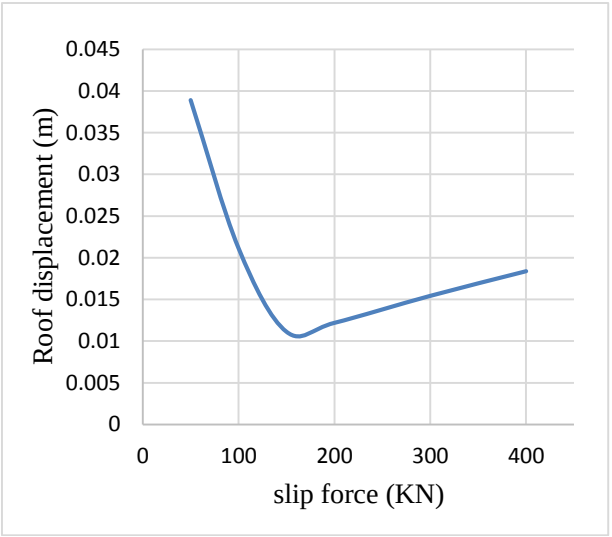

Fig. 7: The graph showing the relationship between roof displacement and slip force

Table 3 depicts the average slip force of seven ground motion records. As can be seen from all frames, the damper's average of slip force was much affected by far-field earthquakes rather than that of near-field.

Table 3. Damper's average of slip force obtaining from ground motion records

Damper's average of slip force obtaining from ground motion records (KN)	4-story building	8-story building	12-story building	16-story building
Far-field earthquake	50	471.4	242.8	357.1
Near-field earthquake	20	185.7	192.8	20

3.2. Hysteresis curve of a cylindrical friction damper

In 2010, Mirtaheri et al [3] tested two cylindrical friction dampers, including A and B. Table 4 represents features of the two experimental models.

Table 4. Features of two samples of cylindrical friction damper

ID	A	B
Sample's slip force (KN)	130	250
D(mm)	100	100
t(mm)	10	10
δ(µm)	100	100
L_0(mm)	49.4	95
Displacement (mm)	50±	50±
Wasting energy in each cycle (KJ)	26	50
Total length (mm)	300	400

In the current research, first, accuracy of the cylindrical friction damper was tested. For this purpose, the force versus displacement graph (hysteresis curve) (figure.8), as well as the pushover curve (figure 9) obtained from OpenSees software were compared to the laboratory sample. The reason for the vertical line at small displacements is that the damper fails to slip when the given force is less than slip force, so it simply slips with a slight displacement. Moreover, regarding the friction damper behavior, the second line would also be almost horizontal. It is clear that the modeled friction damper showed a promising accuracy as compared with experimental results [20-22].

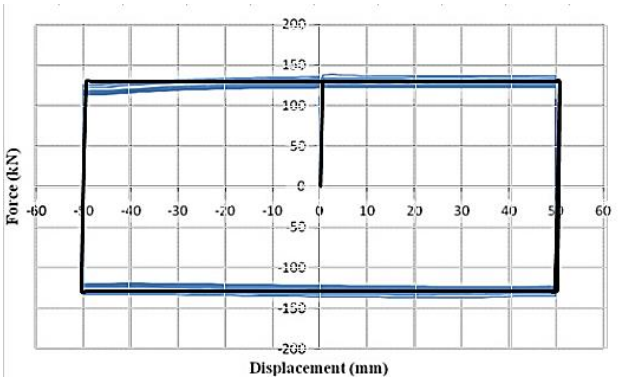

Fig. 8: damper's hysteresis curve [20].

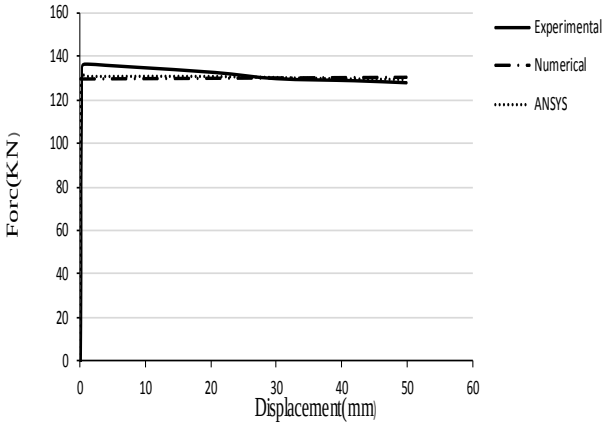

Fig. 9: damper's pushover graph [20].

3.3. Comparing incremental dynamic analyses in the absent of damper

As shown in figures 10, 11, 12, and 13, the horizontal axis depicts relative displacement of the roof, which is higher than other floors. In the current study, comparing graphs showed that, in the absence of a damper, the structure affected by a near-field earthquake collapses with slower acceleration than the one affected by far-field earthquake.

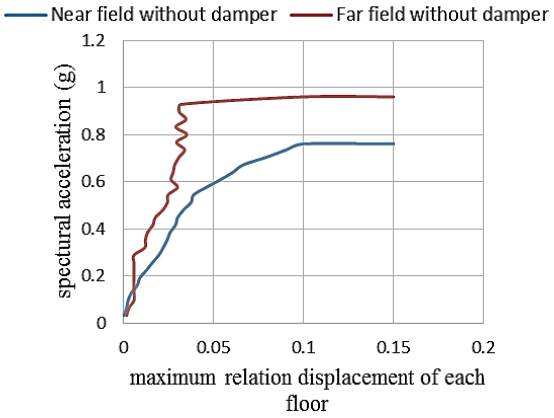

Fig. 10: Comparing spectral acceleration of a four-story structure during far and near-field earthquakes

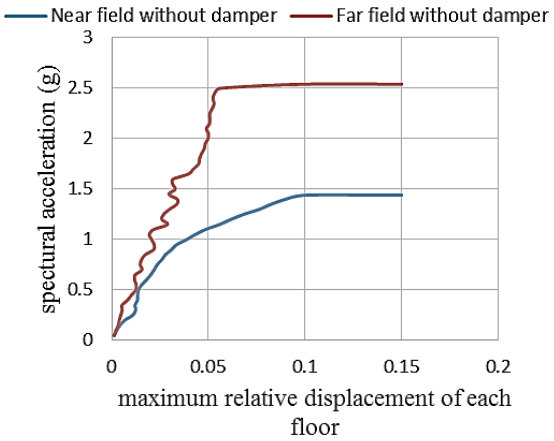

Fig. 11: comparing spectral acceleration of an eight-story structure during far and near-field earthquakes

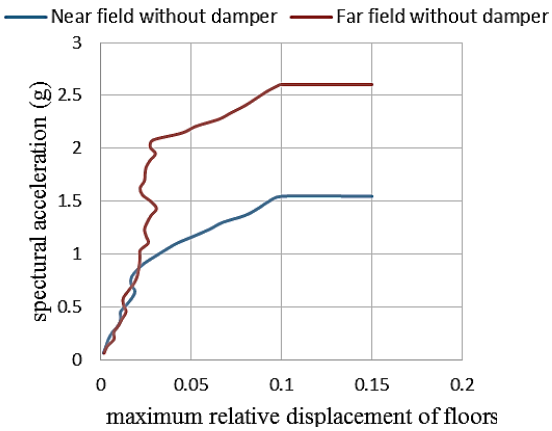

Fig. 12: comparing spectral acceleration of a twelve-story structure during far and near-field earthquakes

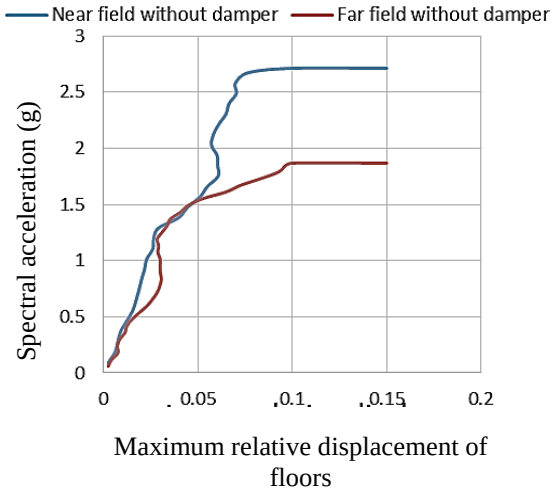

Fig. 13: comparing spectral acceleration of a sixteen-story structure during far and near-field earthquakes

As can be seen from figures 14, 15, 16, and 17, in the presence of a damper and a near-field earthquake, the magnitude of acceleration exerted over each floor in 12 and 16-story structure were compared.

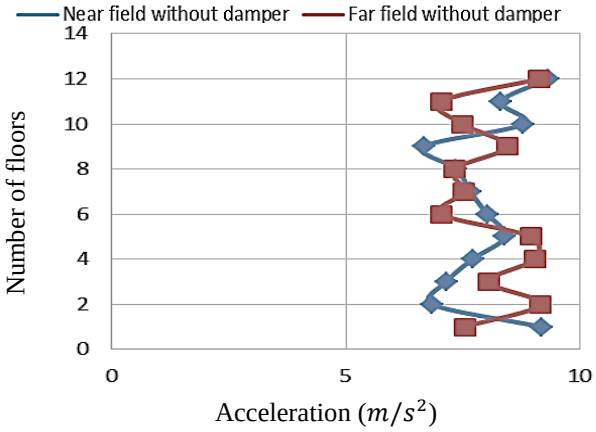

Fig. 14: comparing acceleration of a 12-story structure in the presence and absence of a damper for a near-field earthquake

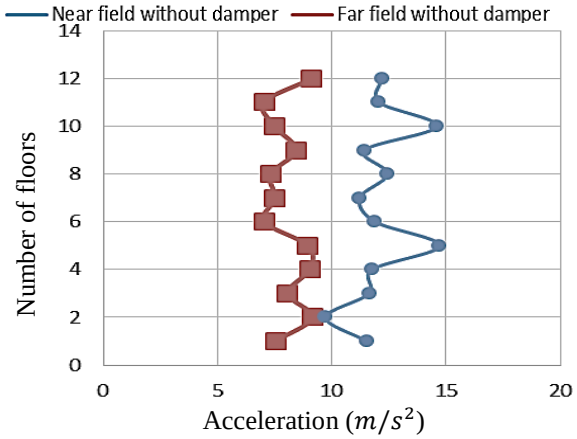

Fig. 15: comparing the acceleration of a 12-story structure in the presence and absence of a damper for a far-field earthquake

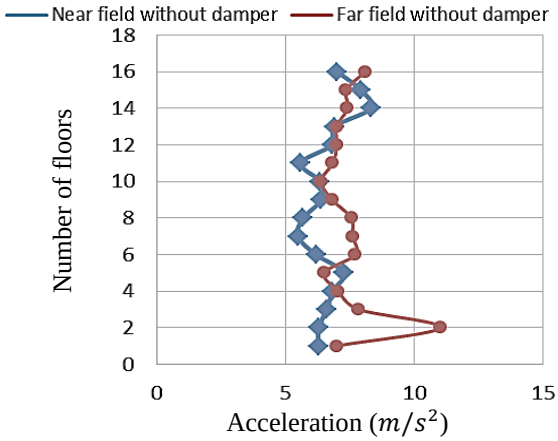

Fig. 16: comparing acceleration of a 16-story structure in the presence and absence of a damper for a near-field earthquake

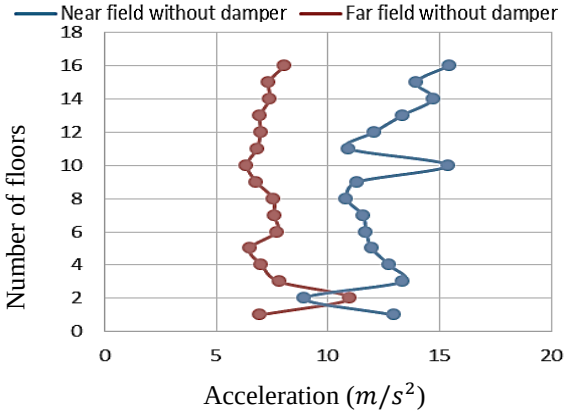

Fig. 17: comparing acceleration of a 16-story structure in the presence and absence of a damper for a far-field earthquake

Figure 14 illustrates the ability of the damper to decrease acceleration over upper floors. Moreover, figure 15 proves that magnitude of acceleration over all floors of a structure in the presence of damper for a near-field earthquake was less than that of a far-field earthquake [23,24]. On the other hand, figure 16 proves that in a near-field earthquake, the magnitude of acceleration over floors of a structure in the presence of a damper was less than the one in the absence of a damper. Furthermore, as can be seen from figure 17, the value of acceleration over all floors of structures with a damper under a near-field earthquake was greater than the one for a far-field earthquake. Table 5 represents changes in maximum acceleration over floors of 12 and 16-story structure for three different conditions.

Table 5. Changes in maximum acceleration over floors of 12 and 16-story structures for three different conditions

Level of changes	maximum acceleration over floors (m/s^2)	Field of earthquake	damper	Number of floors
0.61	5.7	Far	+	12
	9.1	Near	+	
0.02	9.3	Near	-	
0.4	7.8	Far	+	16
	11.0	Near	+	
0.1	12.1	Near	-	

As can be observed from table 8, acceleration of a near-field earthquake over floors of the structure in the presence of the damper showed a decrease compared to acceleration in the absence of a damper. All things being equal, the value of acceleration over floors of a structure during a near-field earthquake showed an increase compared with the one during a far-field earthquake.

3.4. Relative displacements of floors

Table 6 illustrates maximum relative drift of floors in the presence of a damper for both near and far-field earthquakes and their ratio in all structures.

Table 6. Maximum relative drift of floors in the presence of a damper for both near and far-field earthquakes and their ratio

Earthquake	4-story structure	8-story structure	12-story structure	16-story structure
Near	0/018	0/013	0/016	0/023
Far	0/004	0/008	0/015	0/009
ratio	4/2	1/7	1/1	2/5

Table 6 proves that maximum relative drift of floors in all structures in the presence of a damper showed an increase for a near-field earthquake compared to the far-field one.

3.5. Graphs concerning the history of roof acceleration, base shear, roof displacement, and roof velocity for a 16-story frame

Figures 18, 19, 20, and 21 compares such factors as roof acceleration, base shear, roof displacement, and velocity for a 16-story frame during a near-field earthquake in the presence and absence of a damper.

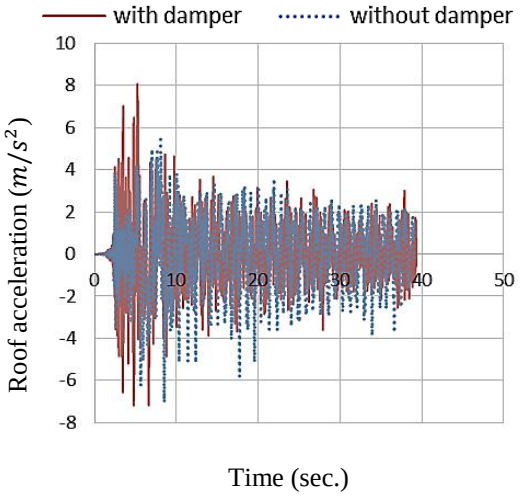

Fig. 18: Roof acceleration for a 16-story frame

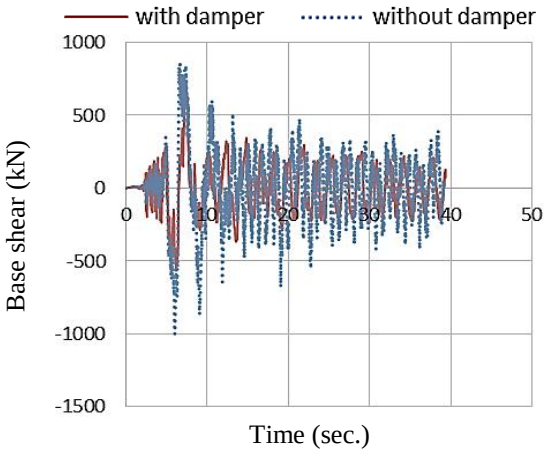

Fig. 19: Base shear for a 16-story frame

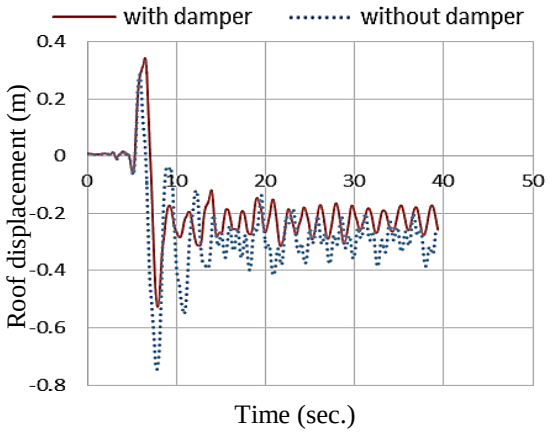

Fig. 20: Roof displacement of a 16-story structure

Figure 18 illustrates a decrease in roof acceleration during a near-field earthquake in the presence of a damper compared with its absence. Figure 19 shows a decrease in base shear during a near-field earthquake in the presence of a damper compared with its absence.

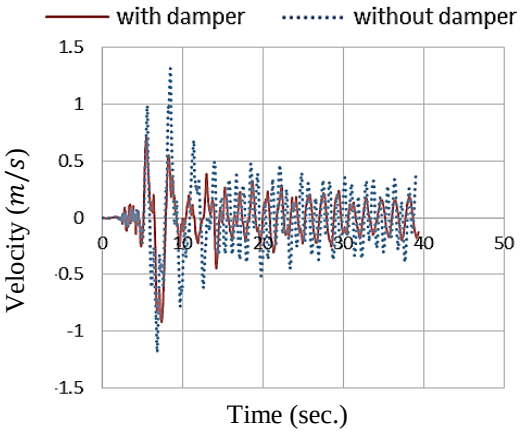

Fig. 21: Roof velocity of a 16-story structure

Figure 20 depicts a decrease in roof displacement in the presence of a damper compared with its absence. Moreover,

Figure 21 illustrates a decrease in roof velocity in the presence of a damper compared with its absence.

From data in table 7, value of four factors such as roof acceleration, roof displacement, roof velocity, and base shear in the presence and absence of a damper, as well as their changes during a near-field earthquake in a 16-story structure are apparent.

Table 7. Comparison between acceleration and base shear, roof displacement, and roof velocity as well as their changes in the presence and absence of a damper

A 16-story structure				
	Acceleration (m/s^2)	Base shear (KN)	Displacement (m)	Velocity (m/s)
In the presence of a damper	5.1	659197.7	0.5	0.9
In the absence of a damper	7.0	998547	0.7	1.3
Level of decrease	3.0	0.3	0.3	0.3

As can be seen from figure 22, the damper located on the first floor of a 16-story structure during a near and far-field earthquake begins to slip with a power of 200 and 350 (KN), respectively. As a result, during a far-field earthquake the structure burdens at maximum 1.5 and 2 cm tension and pressure, respectively. However, all things being equal, displacement of the structure would be at maximum 1 cm during both near and far-field earthquakes. As it is apparent, during a near-field ground motion record the damper experienced the least slip and the most displacement.

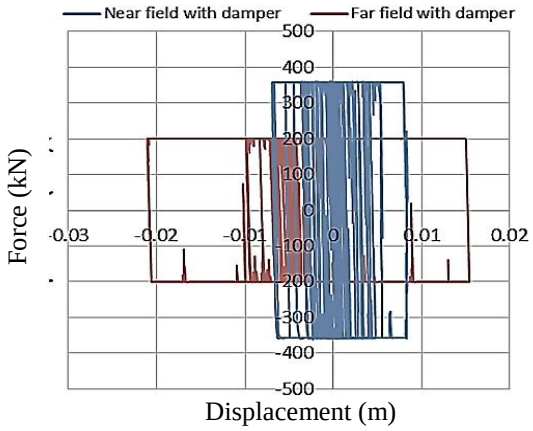

Fig. 22: Comparison between hysteresis curves of a damper during a near-field earthquake and a far-field earthquake at the first floor of a 16-story structure

3.6. Comparing base shear in the four given structures

Values concerning base shear for all four structures are available in Table 4. From this data, we can see that in the presence of a damper in all structures, a far-field earthquake resulted in greater base shear. Moreover, all things being equal, structures burden less base shear in the presence of a damper.

Table 8. Maximum base shear

Maximum base shear (KN)	Earthquake field	Existence of a Damper	Number of floors
689.2	Far	yes	4
314.7	near	yes	
957	Far	no	
764.4	near	no	
895.8	Far	yes	8
555.1	near	yes	
962.9	Far	no	
1111.0	near	no	
821.8	near	yes	12
۹68.2	Far	no	
1153.5	near	no	
1331.4	Far	yes	
۳96.7	near	yes	16
۲65.9	Far	no	
1505.4	near	no	
998.5	Far	yes	

Figures 23 and 24 compare spectral velocity of a 16-story structure.

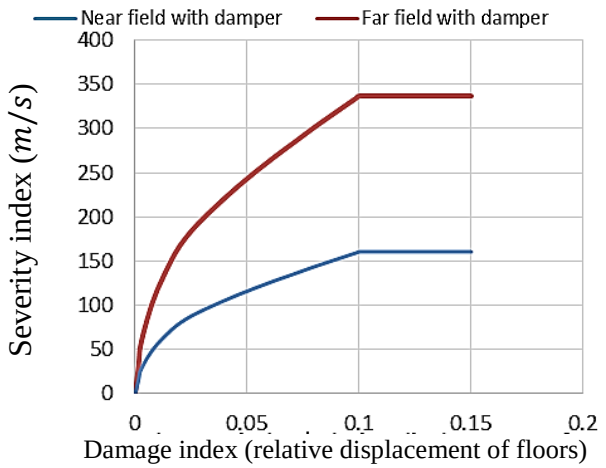

Fig. 23: Comparing SV parameter of a structure in the presence of a damper during a near-field earthquake with the one during a far-field earthquake

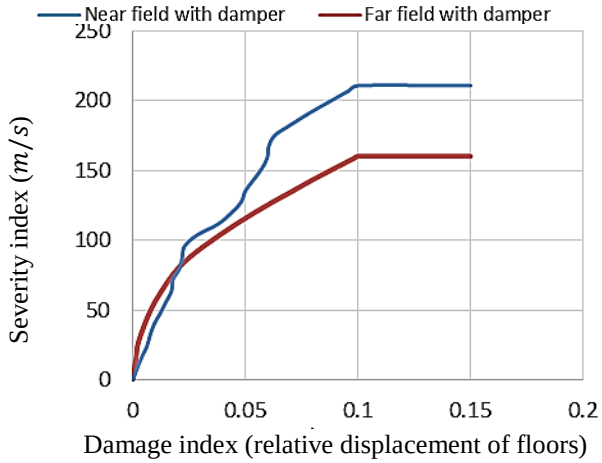

Fig. 24: Comparing SV parameter of a structure during a near-field earthquake in the presence of a damper with the one in the absence of a damper

As can be seen from figure 23, in the presence of a damper the structure collapses with lower velocity during a near-field earthquake compared to a far-field one. The graph indicates that near-field earthquakes are highly destructive than far-field ones. Figure 24 depicts that during a near-field earthquake a structure collapses with higher velocity in the presence of a damper compared to its absence. As a result, both figures 23 and 24 acknowledge the efficiency and beneficial impact of dampers.

4. Conclusion

This research presents a comparative study to assess the near- and far-field seismic performance of cylindrical friction damper. The following results are derived from this research:

- During near or far-field earthquakes, average acceleration over floors of the structures in the presence of a damper was 0.92 greater than the ones in the absence of a damper. During near-field earthquakes, in the presence or absence of a damper, average acceleration over floors of the structures was 1.63 greater than those obtained during far-field earthquakes.
- During a near-field earthquake, average relative displacement of floors in the absence of a damper was 1.84 greater than those in the presence of a damper. In addition, the average relative displacement of roofs in the presence of a damper was 0.82 greater than those in the absence of a damper.
- The average velocity of the roof story of the given structures during a near-field earthquake in the presence of a damper was 0.78 greater than the ones in its absence. The average dissipated energy by the damper during a near-field earthquake was almost 0.77 greater than the ones during a far-field earthquake.
- The average slip forces of the damper during a near-field earthquake was close to 0.3 greater than the ones obtained during a far-field earthquake. Also, the average displacement of the damper during a near-field earthquake was close to 2.6 greater than the ones obtained during a far-field earthquake.

References

[1] Zafarani Hamid& Noorzd Asadollah & Bargi Khosro (2006) (*Generation Of Near-Field Ground Motions In Tehran From Future Large Earthquake In The Alborz Seismic Zone*) First European Conference on Earthquake Engineering and Seismology (a joint event of the 13th ECEE & 30th General Assembly of the ESC)Geneva, Switzerland.

[2] Khaloo Ali R. & Khosravi Horr (2006) (*Studying Shear and Flexural Response of Buildings to Pulse like Ground Motion in Near-Field Earthquakes*) First European Conference on Earthquake Engineering and Seismology (a joint event of the 13th ECEE & 30th General Assembly of the ESC) Geneva, Switzerland.

[3] Mirtaheri Masoud, Zandi Amir Peyman & Sharifi Samadi Sahand & Rahmani Samani Hamid (2010) "*Numerical and experimental study of hysteretic behavior of cylindrical friction dampers*" Journal of Engineering structure.

[4] S. Mazzoni, F. McKenna, M.H. Scott, G.L. Fenves, B. Jeremic. (2004) (*OpenSees Command Language Manual*).

[5] Pall AS, Marsh C. Response of friction damped braced frames. J Struct Eng 1982; 108(9):1313–23.

[6] Wua B, Zhanga J, Williamsb MS, Oua J. Hysteretic behavior of improved Palltyped frictional dampers. Eng Struct 2005;27:1258–67.

[7] Aiken ID, Kelly JM. Earthquake simulator testing and analytical studies of two energy-absorbing systems for multistory structures. Report no. UCB/EERC90/03. Berkeley (CA): Earthquake Engineering Research Center. University of California; 1990.

[8] Nims DK. et al. Application of the energy dissipating restraint to buildings. In: Proc. ATC 17-1 on seismic isolation, energy dissipation, and active control. 1993. p. 627–38.

[9] Ahmad, N. and Masoudi, M., 2020. Eccentric steel brace retrofit for seismic upgrading of deficient reinforced concrete frames. Bulletin of Earthquake Engineering, pp.1-35.

[10] Ahmad, N., Shakeel, H. and Masoudi, M., 2020. Design and development of low-cost HDRBs seismic isolation of structures. Bulletin of Earthquake Engineering, 18(3), pp.1107-1138.

[11] Lavan, O. and Amir, O., 2014. Simultaneous topology and sizing optimization of viscous dampers in seismic retrofitting of 3D irregular frame structures. Earthquake engineering & structural dynamics, 43(9), pp.1325-1342.

[12] BHRC (Building and Housing Research Center). 2004. Iranian Code of Practice for Seismic Resistant Design of Buildings. Standard No. 2800, 3rd edn. BHRC: Tehran.

[13] OpenSees.berkeley.edu(2006). *Steel 01 Material.* [OpenSees.berkeley.edu/OpenSees/manuals/comparisonManual/2770.htm]

[14] Masoudi, M. and Khajevand, S., 2020. Revisiting flexural overstrength in RC beam-and-slab floor systems for seismic design and evaluation. Bulletin of Earthquake Engineering, 18(11), pp.5309-5341.

[15] Chopra A.K.(2000) , " *Dynamics of Structure* : *Theory and Application to Earthquake Engineering*" , Upper saddle river , NJ , (2nd Ed).

[16] Mirtaheri, M., Emami, F., Zoghi, M.A. and Salkhordeh, M., 2019. Mitigation of progressive collapse in steel structures using a new passive connection. Structural Engineering and Mechanics, 70(4), pp.381-394.

[17] Karami-Mohammadi, R., Mirtaheri, M., Salkhordeh, M. and Hariri-Ardebili, M.A., 2020. Vibration Anatomy and Damage Detection in Power Transmission Towers with Limited Sensors. Sensors, 20(6), p.1731.

[18] Karami-Mohammadi, R., Mirtaheri, M., Salkhordeh, M., Mosaffa, E., Mahdavi, G. and Hariri-Ardebili, M.A., 2019. Seismic mitigation of substation cable connected equipment using friction pendulum systems. Structural Engineering and Mechanics, 72(6), pp.785-796.

[19] Rahmani Samani Hamid, Mirtaheri Masoud, Zandi Amir Peyman (June 2015). *Experimental and numerical study of a new adjustable frictional damper*. Journal of Constructional Steel Research.

[20] Mirzaeefard Hamid, Mirtaheri Masoud (1394). *Evaluation of Seismic Behavior and Select Optimal Situation of Cylindrical Frictional Dampers in Steel Structures*. Journal of structural and construction engineering.

[21] Mirtaheri, M. and Salkhordeh, M., 2018. *A real-time recursive dynamic model for vehicle driving simulators.* Journal of Numerical Methods in Civil Engineering, 3(2), pp.13-23.

[22] Samani, H.R. and Mirtaheri, M., 2016. *Seismic response sensitivity of the structures equipped with cylindrical frictional dampers to the value of slippage load.* Journal of Numerical Methods in Civil Engineering, 1(1), pp.57-63.

[23] Alavi, B. and Krawinkler, H., 2001. Effects of near-fault ground motions on frame structures (p. 301). Stanford: John A. Blume Earthquake Engineering Center.

[24] Fanaie, N., Sadegh Kolbadi, M. and Afsar Dizaj, E., 2017. *Probabilistic Seismic Demand Assessment of Steel Moment Resisting Frames Isolated by LRB*. Journal of Numerical Methods in Civil Engineering, 2(2), pp.52-62.